

Development of a novel artifact-free eye shield based on silicon rubber-lead composition in the CT examination of the head

Yulia Irdawati¹, Heri Sutanto¹ , Choirul Anam¹ ,
Toshioh Fujibuchi², Fatimatuz Zahroh¹ and
Geoff Dougherty³

¹ Department of Physics, Faculty of Sciences and Mathematics, Diponegoro University, Jl. Prof. Soedarto SH, Tembalang, Semarang 50275, Central Java, Indonesia

² Department of Health Sciences, Faculty of Medical Sciences, Kyushu University, 3-1-1 Maidashi, Higashi-ku, Fukuoka 812-8582, Japan

³ Department of Applied Physics and Medical Imaging, California State University Channel Islands, Camarillo, CA 93012, United States of America

E-mail: herisutanto@fisika.undip.ac.id

Received 29 May 2019, revised 23 June 2019

Accepted for publication 4 July 2019

Published 24 September 2019



CrossMark

Abstract

The aim of this work was to develop a novel artifact-free eye shield and evaluate its effect on the dose received by the eye lens and the resulting image quality in the CT examination of the head. A new material for an eye shield was synthesised from silicon rubber (SR) and lead (Pb) using a simple method. The percentage of Pb was varied from 0 to 5% wt. An anthropomorphic head phantom was scanned with and without the SR-Pb eye shield, and compared with a tungsten paper (WP) eye shield. The distance from the eye shield and head was varied from 0 to 5 cm. The dose to the eye lens was measured using photo-luminescence detectors (PLDs). The presence of artifacts was determined by measuring CT numbers at different eye lens locations and by subtracting images with and without the eye shield. The dose reduction increases with increasing Pb content in the SR-Pb eye shield. A 5% wt SR-Pb eye shield reduced the eye lens dose by up to 50%, whereas the WP eye shield reduced the dose by up to 86%. The CT numbers in images with the SR-Pb eye shield in the regions of both eyes and the center of the head phantom is similar to those without the eye shield, indicating that there is no artifact in the resulting image. Using the WP eye shield, there is considerable artifact with the CT number increasing by up to 700% in the regions of both eyes and the center of the head. It is found that the distance between the SR-Pb eye shield and the

head does not affect either the dose or the resulting images. A SR-Pb-based eye shield can be applied in clinical environments and should be placed directly above the eye surface for dose optimisation.

Keywords: silicone rubber, eye shield, CT scan, artifact free, head CT examination

(Some figures may appear in colour only in the online journal)

Introduction

The eye lens is highly sensitive to ionizing radiation in the head area [1]. Due to the frequent use of CT scans in examinations of the head [2], it is important to keep the dose to the eye lens as low as possible to prevent deterministic effects such as cataracts [3, 4]. The International Commission on Radiological Protection (ICRP) reported that the dose threshold to avoid cataracts is about 500 mGy [5, 6]. The eye lens dose received by patients in a head CT scan is far lower, at about 50 mGy [7–9]. However efforts to reduce the eye dose to minimise the risk should be still be practiced [10]. Based on data from the World Health Organization (WHO) [11], cataracts are one of the biggest causes of visual impairment and blindness in the world. A dose reduction to the eye lens usually causes a deterioration in image quality [12]. Therefore, dose optimisation is needed for proper diagnosis consistent with radiation protection.

There are many techniques that can be used to optimise dose to the eye, including gantry angulation, mis-centering, tube current modulation (TCM), and using eye shields. Many studies reported that gantry angulation can reduce the eye lens dose by up to 80% [13–15], but it causes artifacts in the image, especially in the posterior fossa. It cannot be applied to all diseases in the head area, such as diseases in the sinus area, orbital and mastoid [10, 16]. Another technique used for eye dose reduction is mis-centering [17–20] where the eye lens is placed above the iso-center, reducing the eye lens dose by up to 30%. However it increases image noise and can result in truncation of the image. A further technique for eye dose reduction is the TCM technique [21, 22]. Many studies reported that using this technique reduced the eye lens dose by up to 50% and no artifact was produced [23, 24]. However not all CT scan devices have TCM features [6].

Another technique that can be used for eye lens dose reduction is using an eye shield. Many types of materials have been developed for this purpose. Ngaile *et al* [25] developed an eye shield from lead-latex, Huggeth *et al* [26] and Seoung [27] used barium-latex, and Liebmann *et al* [28], Mendes *et al* [29] and Lai *et al* [30] used bismuth-latex. All of these materials significantly reduced the eye lens dose, but the quality of the images deteriorated because of artifacts that covered the eye lens. Artifacts are mainly due to materials that have a high atomic number (Z) [31]. To minimise artifacts in the resulting image, Young *et al* [32], McCollough *et al* [33] and Inkoom *et al* [34] increased the distance between the eye shield and eye.

Developing a novel eye shield that is able to significantly reduce the eye lens dose and minimise the appearance of artifacts is very important. Jaya and Sutanto [35] reported that silicone rubber (SR) of thickness 1 cm could be used as a radiation filter in digital radiography (DR) and absorbs radiation up to 59.9%, and Mehnati *et al* [36] reported using 1 mm thick bismuth-silicon with 10% bismuth during chest CT can reduce the dose to the breast by 12% and results in lower noise. We hypothesise that the SR and lead (Pb; $Z = 82$) material may be

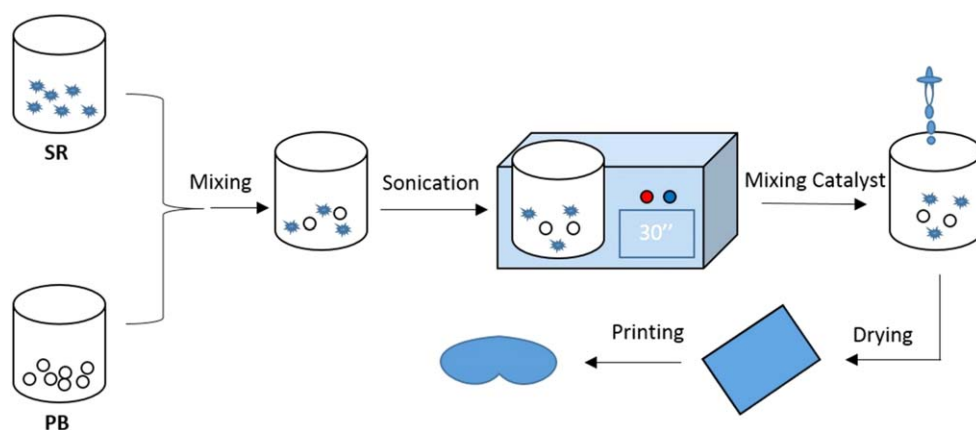


Figure 1. Synthesis of the SR-Pb eye shield.

an effective eye shield in head CT examinations. SR is a synthetic polymer so that its elasticity may be maintained even if Pb is added, so that it can have sufficient flexibility to cover the eye region [37, 38]. We made a SR-Pb eye shield and evaluated the effect of adding various percentages of Pb, the effect of the distance between the eye shield and the head, and the image quality of the resulting image.

Materials and methods

Synthesis of the novel eye shield

The synthesis of the eye shield is shown in figure 1. It was constructed from SR-RTV52 and lead (II) acetate trihydrate ($\text{Pb}(\text{CH}_3\text{COO})_{2-3}\text{H}_2$). Synthesis of SR-Pb was started by mixing the SR with Pb of various percentages (0% wt, 1% wt, 2% wt, 3% wt, 4% wt, and 5% wt). The mixing process was completed in 30 min. The mixture was then sonicated in an ultrasonic bath for 30 min to accelerate homogenisation. After that, it was mixed with a 3.5 ml Bluesil catalyst to accelerate the drying process for 6 min. After drying, the eye shield was printed with a dimension of $17 \times 17 \times 0.6 \text{ cm}^3$. It can be customised into a specific shape, such as a pair of glasses.

Dose measurement

Photo-luminescence detectors (PLDs) (type GD-352M, Chiyoda Technol Corporation, Japan) were used to evaluate the effect of the eye shield to the eye lens dose in a head CT scan. The PLDs were calibrated by simultaneous irradiation with a 0.6 cc cylindrical ionisation dosimeter using x-rays of 120 kVp, at half-value layer 4.8 mm Al from a radiography source. The air kerma at calibration was 1.81 mGy with an uncertainty of 1.84%. They were then placed above the surface of the eyes on the head phantom. 3 PLDs were used for the right eye and 3 PLDs were used for the left eye, as shown in figure 2. The doses were then read by the Dose Ace (type FDG-1000, Chiyoda Technol Corporation, Japan). The PLDs were read before and after scanning. In addition, the effect of distance between the eye shield and the eye (0 cm, 1 cm, 2 cm, 3 cm, 4 cm and 5 cm) was evaluated. A Toshiba Alexion 4-slice helical CT

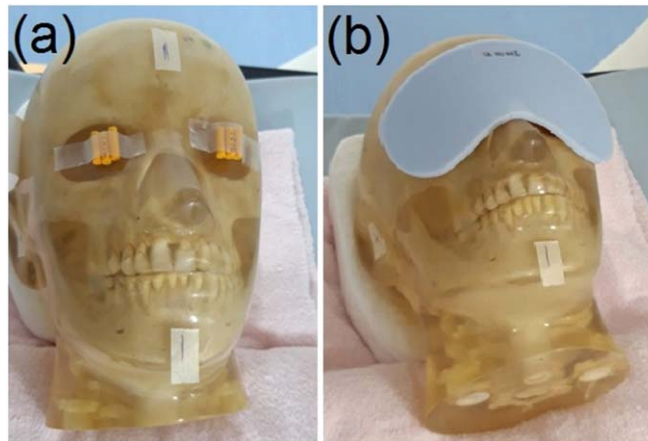


Figure 2. (a) PLDs were placed above the surface of the eye on the head phantom, and (b) the eye shield was placed above the head phantom. The distance between the eye shield and the head phantom was varied from 0 cm to 5 cm.

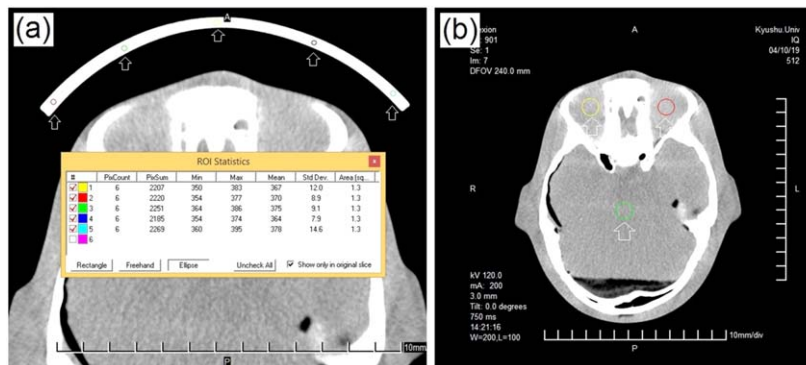


Figure 3. (a) Positions of the ROIs to calculate HU of the SR-Pb eye shield and its homogeneity. The size of the ROIs was 6 pixels or about 1.3 mm². (b) Positions of the ROIs to characterise the amount of artifact by determining HU values in the eye area and the center of the head. The size of the ROIs was 460 pixels or around 100 mm².

scanner was used with exposure parameters of: tube voltage of 120 kVp, tube current of 100 mA, time rotation of 0.75 s, field of view (FOV) of 24 cm, and slice thickness of 8 mm.

Image characteristic of the SR-Pb and image quality

To determine the image characteristic of the developed SR-Pb, the radiodensity (Hounsfield units (HU)) of the eye shield and its homogeneity were measured. Five regions of interest (ROIs) were constructed in the image of the SR-Pb, as shown in figure 3(a). The five ROIs were in the form of a circle with a size of 1.3 mm² or 6 pixels. The size of ROI appeared too small because it is limited to the thickness of the SR-Pb eye shield, which is only 6 mm. The distance between adjacent pixels for 240 mm field of view (FOV) was 0.468 mm. To ensure a homogeneous ROI on the eye shield, the maximum number of pixels that included the circular ROI, therefore, was limited to only 6 pixels. If the size of the ROI is greater than that

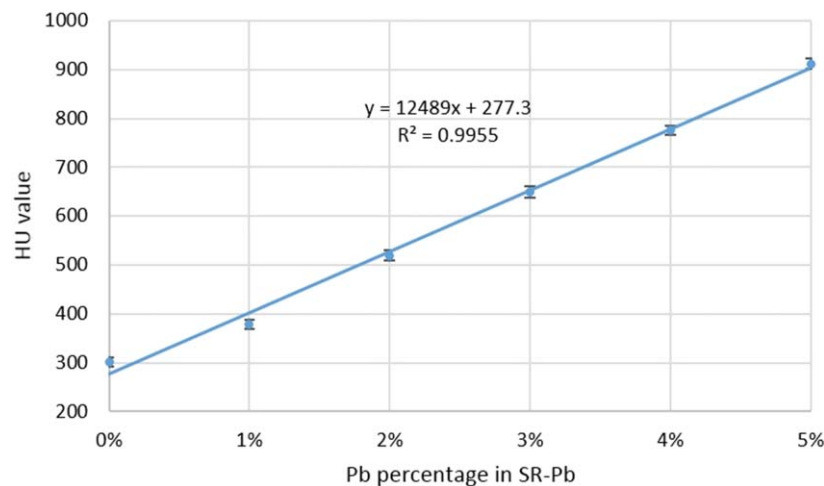


Figure 4. Graph of the relationship between Pb percentage at the eye shield and HU value.

size, it is possible that the ROI is no longer homogeneous because it has included pixels in the edge area of the eye shield. In the ROIs, the mean values of HU and standard deviation of HU were measured. The measurements were performed for variations of the Pb percentage in the SR-Pb eye shield. The homogeneity of the SR-Pb was calculated by equation (1).

$$H = \left(1 - \frac{|HU_{\max} - HU_{\min}|}{HU_{\min}} \right) \times 100\%. \quad (1)$$

The absence of artifact was indicated by no change in HU and its standard deviation with and without the SR-Pb eye shield. The mean value of HU and its standard deviation in the left eye area and right eye area were calculated, as shown in figure 3(b). The ROIs in the right eye and left eye were circular with a size of around 100 mm^2 or 460 pixels. If the artifact was large, it may reach the center of the image. Therefore, the change of HU value in the center of the image was also observed.

The existence of the artifact can be evaluated more comprehensively by subtracting two images, one with the SR-Pb eye shield and one without it. The effect of variations in the percentage of Pb in the eye shield and distance (0–5 cm) between the eye shield and the patient head were measured.

Results

Characteristic of the SR-Pb eye shield

The SR-Pb eye shield was made with various percentages of Pb from 0 to 5% by weight. There was a linear relationship between Pb percentage and HU value in the image, with $R^2 > 0.99$, as shown in figure 4. The homogeneity of the eye shield SR-Pb was evaluated by measuring the HU values at five areas in the eye shield images. The HU values for five areas with variations of Pb percentage is tabulated in table 1. The homogeneities of HU are more than 90% for all Pb contents from 0 to 5% by weight.

Table 1. The homogeneity of HU values in the SR-Pb eye shield for variations of Pb percentage.

Pb percentage	HU value					Homogeneity (%)
	Left edge	Center left	Center	Center right	Right edge	
0% wt	309 ± 4.8	296 ± 14.2	294 ± 8.3	297 ± 7.2	310 ± 8.5	94.6
1% wt	373 ± 5.4	381 ± 8.1	367 ± 12.0	377 ± 12.2	399 ± 9.8	91.3
2% wt	526 ± 5.3	518 ± 11.3	509 ± 11.4	514 ± 11.1	532 ± 8.5	95.5
3% wt	640 ± 12.4	650 ± 12.1	652 ± 10.8	644 ± 13.9	659 ± 8.4	97.0
4% wt	780 ± 12.4	774 ± 6.4	760 ± 6.1	774 ± 12.8	794 ± 7.8	95.5
5% wt	897 ± 11.2	927 ± 10.9	909 ± 11.9	895 ± 10.5	929 ± 9.8	96.2

996

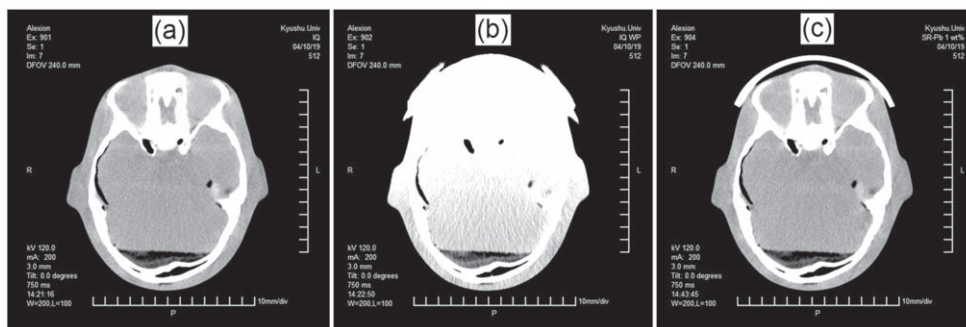


Figure 5. (a) Original image of the head phantom, (b) image of the head phantom using the WP eye shield, and (c) image of the head phantom using the SR-Pb 1% wt eye shield.

Table 2. HU value and its standard deviation on the right eye, left eye and center of the head phantom before the use of the eye shield, use of the WP eye shield and the use of the SR-Pb 1% wt eye shield.

Variation	Left eye		Right eye		Center of head	
	Mean HU	SD of HU	Mean HU	SD of HU	Mean HU	SD of HU
Without eye shield	139	6.6	140	6.0	122	6.8
WP	1166	258.9	1012	205.1	185	17.1
SR-Pb 1% wt	136	6.7	138	7.4	122	8.2

Comparison of the eye shields

The images of the head phantom in the orbital area with and without the SR-Pb eye shield are shown in figure 5. The original image without the eye shield is shown in figure 5(a). Figure 5(b) shows the image of the head phantom with a tungsten paper (WP) eye shield supplied by Toppan Printing and Kyoto University, and figure 5(c) shows the image of the head phantom with the SR-Pb 1% wt eye shield. Figure 5 shows many artifacts in the image of the head phantom with the WP eye shield, but none with the SR-Pb eye shield.

The HU value and its standard deviation in the left eye, right eye and center of head phantom region are tabulated in table 2. The WP eye shield causes an artifactual increase in HU value of more than 700% in the eye region, while the SR-Pb eye shield causes no significant artifact.

SR-Pb eye shield with variation of Pb percentage

The percentage of Pb in the SR-Pb eye shield was varied from 0% to 5% by weight. Surface doses of eyes with and without the SR-Pb eye shield with various Pb percentages, are shown in figure 6. The dose to the eye lens without the eye shield is about 63.5 ± 2.1 mGy, and the doses decrease by 6.1, 31.6, 35.3, 42.5, 43.5 and 50.0% for Pb percentages of 0, 1, 2, 3, 4, and 5% wt, respectively. The doses to the right and left eye are very similar.

Images of the head phantom with the SR-Pb eye shield at various Pb percentages are shown in figure 7. There are no visible artifacts in the eye region for Pb percentages from

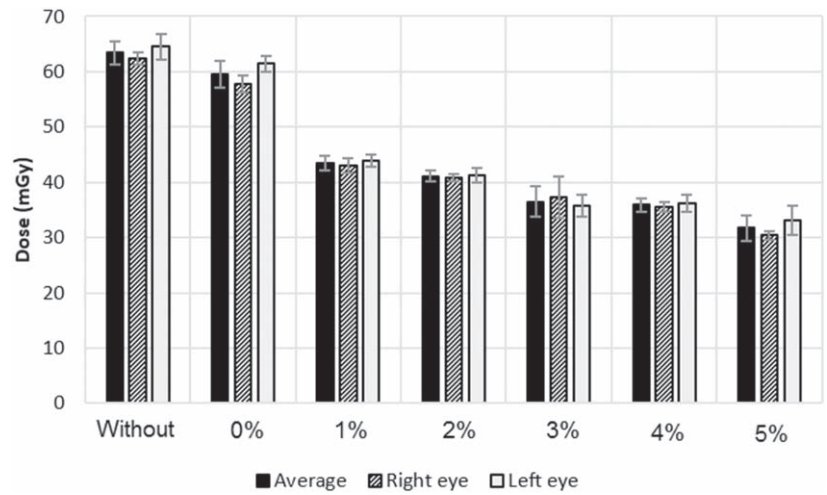


Figure 6. Surface doses of eye with and without the SR-Pb eye shield with various Pb percentages from 0 to 5% wt. The standard deviations are shown by bars.

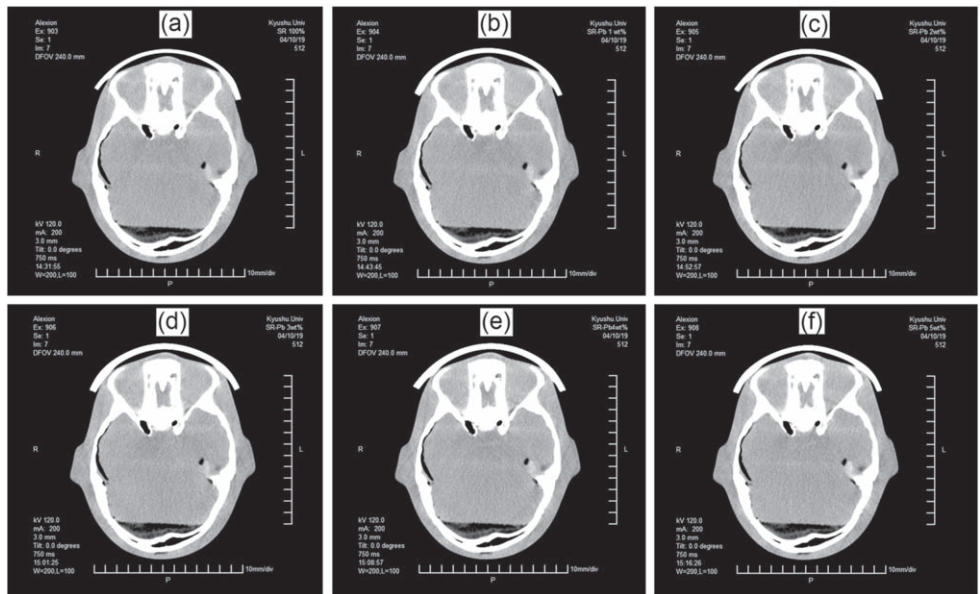


Figure 7. Images of head phantom for various Pb percentages with the SR-Pb eye shield. (a) 0 (b) 1 (c) 2 (d) 3 (e) 4 and (f) 5% wt. The SR-Pb eye shields are on the head.

0%–5% wt. Subtraction was used to identify any subtle artifacts. The results of subtraction between the images with and without the SR-Pb eye shield, for various Pb percentages, are shown in figure 8. These subtraction images show only slight artifacts at the end of the SR-Pb eye shield, and artifacts outside the head which do not affect the image of the head itself.

The HU values and their standard deviations in the region of both eyes and at the center of the head are tabulated in table 3. This shows that there is no significant change in the HU

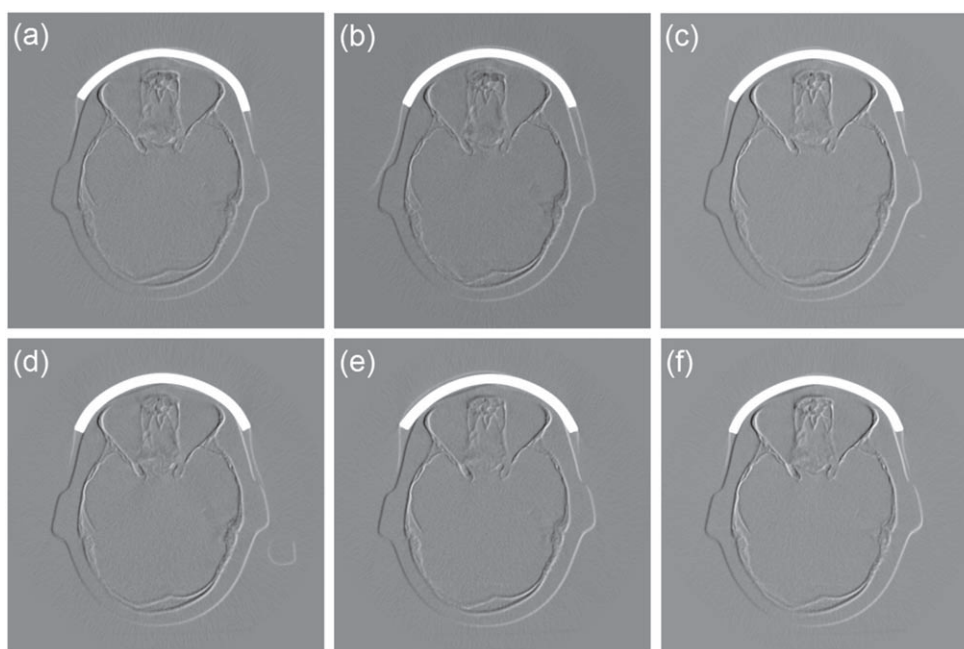


Figure 8. Result of subtraction images with and without the SR-Pb eye for various Pb percentages; (a) 0, (b) 1, (c) 2, (d) 3, (e) 4, and (f) 5% wt. The SR-Pb eye shields are on the head.

Table 3. HU value and standard deviation in the left eye region, right eye region and center of the head phantom using the SR-Pb eye shield with various Pb percentages (0 to 5% wt).

Pb percentage (% wt)	Left eye		Right eye		Center of head	
	Mean HU	SD of HU	Mean HU	SD of HU	Mean HU	SD of HU
0	138	9.0	135	6.9	123	7.9
1	136	6.7	138	7.4	122	8.2
2	137	7.4	135	6.8	119	7.0
3	138	7.9	138	6.3	120	6.2
4	139	8.2	134	6.1	122	7.2
5	134	8.0	133	7.1	122	7.5

values or their standard deviations for variations in Pb percentage from 0 to 5% wt. The difference in HU values is in the range of image noise.

Variation due to the distance of the SR-Pb eye shield to head phantom

Although the SR-Pb eye shield does not cause significant artifact, the distance between the SR-Pb eye shield and the head phantom may have an effect. We varied the distance from 0 to 5 cm using a cork placed between the SR-Pb eye shield and head at a Pb percentage of 5% wt.

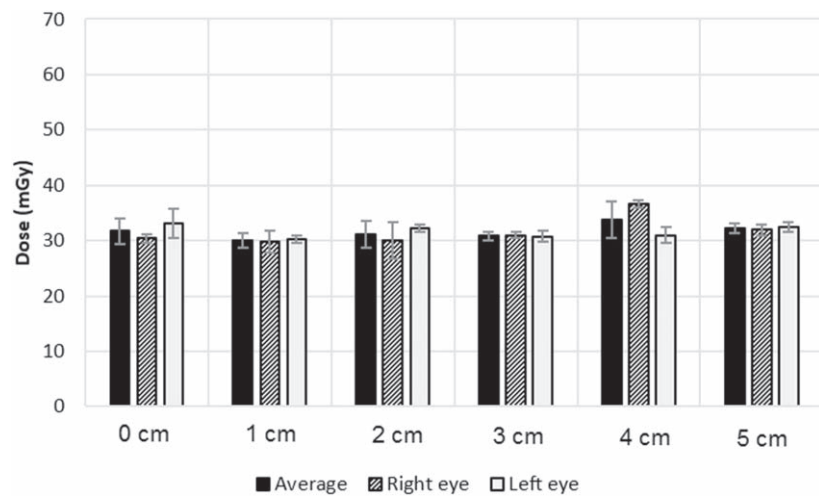


Figure 9. Surface doses at the eyes using the SR-Pb 5% wt eye shield for distances from 0 to 5 cm.

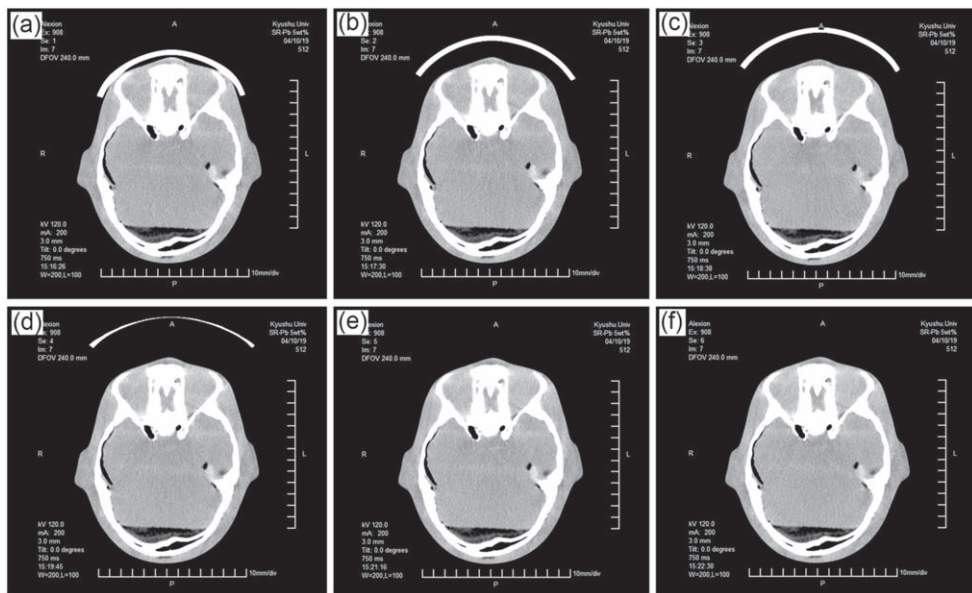


Figure 10. Image of head phantom for various distances for the SR-Pb 5% wt eye shield; (a) 0, (b) 1, (c) 2, (d) 3, (e) 4, and (f) 5 cm.

The respective doses at the surface of the eyes are shown in figure 9. No significant changes in eye dose for distance variations from 0 to 5 cm were observed.

Images of the head phantom with a SR-Pb 5% wt eye mask and variable distances are shown in figure 10. The eye shields do not appear in the images for distance 4 cm and 5 cm, because they are out of the field of view (FOV). Figure 10 shows no changes of image quality and no artifacts for the various distances. Subtraction images (figure 11) confirm that there is

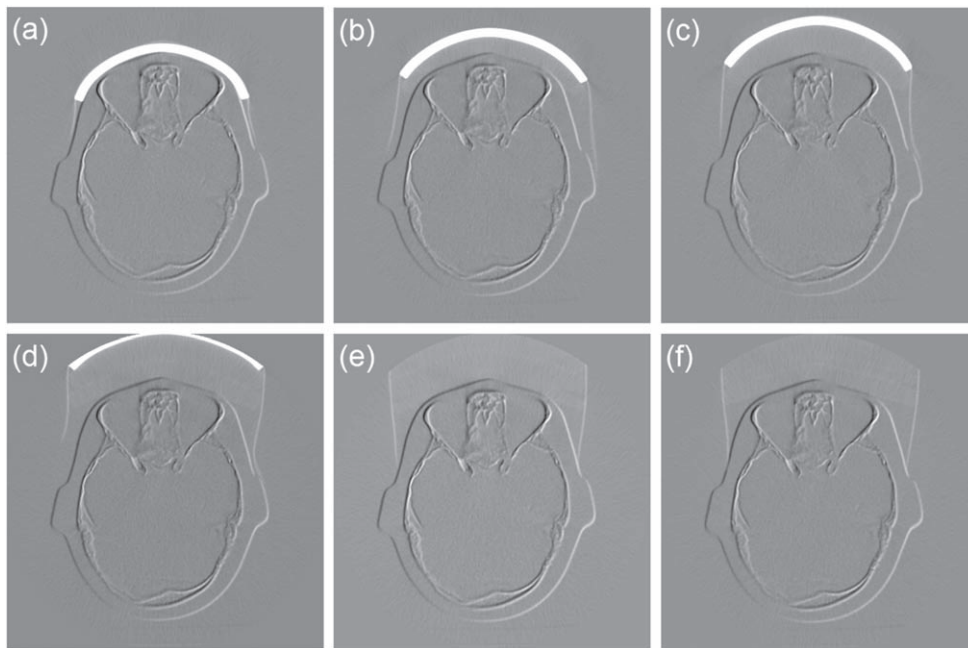


Figure 11. Subtraction images between images with the SR-Pb 5% wt eye shield and images without it for various distances: (a) 0, (b) 1, (c) 2, (d) 3, (e) 4, and (f) 5 cm.

Table 4. HU value and standard deviation in the left eye region, right eye region and the center of head phantom for images with the SR-Pb 5% wt eye shield for distances from 0 to 5 cm.

Distance (cm)	Left eye		Right eye		Center of head	
	Mean HU	SD of HU	Mean HU	SD of HU	Mean HU	SD of HU
0	134	8.0	133	7.1	122	7.5
1	135	8.0	133	6.3	122	8.1
2	138	7.4	136	6.6	122	7.1
3	135	7.4	136	6.7	121	7.8
4	136	8.0	137	7.3	122	7.9
5	138	6.3	137	7.4	121	7.7

no significant artifact, other than a slight artifact at the end of the eye shield. The HU values and their standard deviations in the eye regions and the center of the head image are tabulated in table 4. This shows that there are no significant differences beyond the level of noise due to distance variations from 0 to 5 cm.

Discussion

As shown in the introduction, many materials have been used as an eye shield such as lead-latex [25], barium-latex [26, 27] and bismuth-latex [28–30]. Although the eye shields of these



Figure 12. SR-Pb 5% wt eye shield elasticity.

materials significantly reduced the dose of eye lens, the resulting images cannot be used to make a diagnosis because of severe artifacts, due to the construction material, which mostly has a high atomic number [10, 26–30]. In this study, an alternative material was developed and tested, in the hope of avoiding artifacts.

We propose a novel eye shield for protecting the eye, while maintaining image quality. The new eye shield was made from the silicon rubber-lead (SR-Pb) and resembles an eye sleep mask. It has a very good homogeneity, and its HU values depend linearly on the Pb percentage (R^2 is more than 0.99). The dose reduction also depends on the Pb percentage, increasing with increasing Pb percentage. For a 5% wt Pb percentage, the eye shield reduced the eye dose by up to 50%.

Our new eye shield is potentially applicable in the clinical setting because it has no significant artifact. Any artifact only appears at the edge of the SR-Pb eye shield and it is outside the image of the patient. The SR-Pb eye shield is very light in weight, so patients will feel comfortable when using it and it is easy to position. It can reduce patient anxiety about receiving radiation in their eye which can cause cataracts.

The eye surface is uneven, so the eye shield should have elastic properties to flexibly cover the eye surface. To achieve this, many studies use latex. However, De Jong *et al* [39] reported that latex has a toxic nature and can easily cause infection in the eye. In this study, we replaced the latex with silicon rubber (SR), which has similar properties to latex but is not toxic. The elasticity of the 5% wt Pb SR-Pb eye shield can be seen in figure 12. Other advantages of the SR-Pb eye shield are the availability of SR and Pb is widespread and they

are easily found in the marketplace. The SR-Pb eye shield is very easily synthesised and the production price is cheaper than previous eye shield materials such as bismuth-latex.

The use of an eye shield on a CT machine equipped with tube current modulation (TCM) may lead to an increase in tube current, if the SR-Pb eye shield is located on the head before the scout scan, resulting in an increased dose in that area. The implementation of the SR-Pb eye shield in TCM is quite interesting and will be explored in a further study.

The results of the current study revealed that the SR-Pb is very promising for an effective eye shield in CT head examinations. However, it should be noted that evaluations of this study have only been carried out on an anthropomorphic phantom. Evaluations need to be performed on patients before it can be used clinically. To confirm that the eye shield does not reduce image quality to the point of misinterpretation, evaluations by expert radiologists will be sought in a forthcoming study.

Conclusions

Eye shields made from the SR-Pb material, with a Pb content up to 5% by weight, have been successfully synthesised and evaluated. The use of the eye shield reduces the dose to the eye lens, and the dose reduction increases with the increase of Pb percentage. At a Pb percentage of 5% wt, the dose decreased by up to 50%. Unlike eye shields that already exists, this new eye shield does not cause artifacts in the eye so it has the potential to be used in a clinical environment. It reduces the dose while maintaining image quality. The dose to the eye lens and image quality did not change significantly for eye-mask distances of 0–5 cm, therefore the eye shield can be placed directly on the surface of the eyes.

Acknowledgments

The authors would like to thank the Ministry of Research, Technology and Higher Education of Republic of Indonesia for funding this research in 2019.

ORCID iDs

Heri Sutanto  <https://orcid.org/0000-0003-3404-0337>

Choirul Anam  <https://orcid.org/0000-0003-0156-6797>

References

- [1] Wang X, Li G, Zhao J, Song Y, Xiao J and Bai S 2019 Verification of eye lens dose in IMRT by MOSFET measurement *Med. Dosim.* **44** 107–10
- [2] Lai N K, Liao Y L, Chen T R, Tyan Y S and Tsai H Y 2011 Real-time estimation of dose reduction for pediatric CT using bismuth shielding *Radiat. Meas.* **46** 2039–43
- [3] Kleiman N J, Stewart F A and Hall E J 2017 *Modifiers of Radiation Effect in the Eye* (New York: Columbia University)
- [4] Young L, Wooton L S, Kalet A M, Gopan O, Yang F, Day S, Banitt M and Liao J J 2019 Dosimetric effect of bolus and lens shielding in treating ocular lymphomas with low-energy electrons *Med. Dosim.* **44** 35–42
- [5] International Commission on Radiological Protection 2007 The 2007 recommendations of the international commission on radiological protection. ICRP publication 103 *Ann. ICRP* **37** 1–332

- [6] Lawrence S and Seeram E 2017 The current use and effectiveness of bismuth shielding in computed tomography: a systematic review *Radiol. Open.* **2** 7–16
- [7] Anam C, Haryanto F, Widita R, Arif I, Dougherty G and McLean D 2016 Estimation of eye radiation dose during nasopharyngeal CT examination for an individual patient *Information (Japan)* **19** 3951–62
- [8] Anam C, Haryanto F, Widita R, Arif I, Dougherty G and McLean D 2017 The impact of patient table on size-specific dose estimate (SSDE) *Australas. Phys. Eng. Sci. Med.* **40** 153–8
- [9] Anam C, Budi W S, Adi K, Sutanto H, Haryanto F, Ali M H, Fujibuchi T and Dougherty G 2019 Assessment of patient dose and noise level of clinical CT images: automated measurements *J. Radiol. Prot.* **39** 783–93
- [10] Wang J, Duan X, Christner J A, Leng S, Grant K L and McCollough C H 2012 Reduction of radiation dose to the eye *Radiology* **262** 191–8
- [11] World Health Organization Blindness and vision impairment prevention (Accessed: 29 May 2019) (<https://who.int/blindness/causes/priority/en/index1.html>)
- [12] Alkhorayef M, Sulieman A, Alonazi B, Al-Nuaimi M, Alduaji M and Bradley D 2019 Estimation of radiation-induced cataract and cancer risks during routine CT head procedures *Radiat. Phys. Chem.* **155** 65–8
- [13] Matsubara K, Koshida K, Noto K, Takata T, Suzuki M, Shimono T, Yumamoto T and Matsui O 2011 A head phantom study for intraocular dose evaluation of 64-slice multidetector CT examination in patients with suspected cranial trauma *Eu. J. Radiol.* **79** 283–7
- [14] Nikupaavo U, Kaasalainen T, Reijonen V, Ahonen S and Kortensniemi M 2015 Lens dose in routine head CT: comparison of different optimization methods with anthropomorphic phantoms *Am. J. Roentgenol.* **204** 117–23
- [15] Yabuuchi H, Kamitani T, Sagiya K, Yamasaki Y, Matsuura Y, Hino T, Tsutsui S, Kondo M, Shirasaka T and Honda H 2018 Clinical application of radiation dose reduction for head and neck CT *Eu. J. Radiol.* **107** 209–15
- [16] Perisinakis K, Raissaki M, Tzedakis A, Theocharopoulos N, Damilakis J and Gourtsoyiannis N 2005 Reduction of eye lens radiation dose by orbital bismuth shielding in pediatric patients undergoing CT of head: a monte carlo study *Med. Phys.* **32** 1024–30
- [17] Habibzadeh M A, Ay M R, Asl A R K, Ghadiri H and Zaidi H 2012 Impact of miscentering on patient dose and image noise in x-ray CT imaging: phantom and clinical studies *Phys. Med.* **28** 191–9
- [18] Perisinakis K, Seimenis I, Tzedakis A, Papadakis A E and Damilakis J 2013 The effect of head size/shape, miscentering and bowtie filter on peak patient tissue doses from modern brain perfusion 256-slice CT: how can we minimize the risk for deterministic effect? *Med. Phys.* **40** 011911
- [19] Kataria B, Sandborg M and Althen J N 2016 Implications of patient centring on organ dose in computed tomography *Radiat. Prot. Dosim.* **169** 130–5
- [20] Anam C, Fujibuchi T, Toyoda T, Sato N, Haryanto F, Widita R, Arif I and Dougherty G 2019 The impact of head miscentering on the eye lens dose in CT scanning: phantoms study *J. Phys.: Conf. Ser.* **1204** 012022
- [21] Anam C, Haryanto F, Widita R, Arif I and Dougherty G 2017 The profile of size-specific dose estimate (SSDE) along the longitudinal axis in CT using tube current modulation (TCM) *Information (Japan)* **20** 377–82
- [22] Anam C, Haryanto F, Widita R, Arif I, Dougherty G and McLean D 2018 Volume computed tomography dose index (CTDIvol) and size-specific dose estimate (SSDE) for tube current modulation (TCM) in CT scanning *Int. J. Radiat. Res.* **16** 289–97
- [23] Duan X, Wang J, Christner J, Leng S, Grant K L and McCollough C H 2011 Dose reduction to anterior surfaces with organ-based tube current modulation: evaluation of performance in a phantom study *Am. J. Roentgenol.* **197** 689–95
- [24] Huang Y, Zhou W, Gao Y and Liu H 2018 Monte carlo simulation of eye lens reduction from CT scan using based tube current modulation *Phys. Med.* **48** 72–5
- [25] Ngaile J E, Uiso C B S, Msaki P and Kunselman A R 2008 Use of lead shields for radiation protection of superficial organs in patients undergoing head CT examinations *Radiat. Prot. Dosim.* **130** 490–8
- [26] Huggett J, Mukonoweshuro W and Loader R 2013 A phantom-based evaluation of three commercially available patient organ shields for computed tomography x-ray examinations in diagnostic radiology *Radiat. Prot. Dosim.* **155** 161–8

- [27] Seoung Y H 2015 Evaluation of radiation dose reduction during CT-scans using oxide bismuth and nano-barium sulfate shields *J. Korean Phys. Soc.* **67** 1–6
- [28] Liebmann M, Lullau T, Kluge A, Poppe B and Boetticher H V 2014 Patient radiation protection covers for head CT scans—a clinical evaluation of their effectiveness *Fortschr. Röntgenstr.* **186** 1022–7
- [29] Mendes M, Costa F, Figueira C, Madeira P, Teles P and Vaz P 2015 Assessment of patient dose reduction by bismuth shielding in CT using measurement, GEANT4 and MCNPX simulations *Radiat. Prot. Dosim.* **165** 175–81
- [30] Lai C W K, Cheung H Y, Chan T P and Wong T H 2015 Reduction the radiation dose to the eye lens region during CT brain examination: the potential beneficial effect of the combined use of bolus and a bismuth shield *Radioprotection* **50** 195–201
- [31] La L B T, Leong Y K, Leatherday C, Au P I, Hayward K and Zhang L C 2016 X-ray protection, surface chemistry and rheology of ball-milled submicron Gd₂O₃ aqueous suspension *Colloids and Surfaces A: Physicochem. Eng. Aspects.* **501** 75–82
- [32] Young H L, Eun T P, Pyong K C, Hyung S S, Bo K J, Sang I S and Kyung S Y 2011 Comparative analysis of radiation dose and image quality between thyroid shielding and unshielding during CT examination of the neck *Am. J. Roentgenol.* **196** 611–5
- [33] McCollough C H, Wang J and Gould R G 2012 The use of bismuth breast shields for CT should be discouraged *Med. Phys.* **39** 2321–3
- [34] Inkoom S, Papadakis A E, Raissaki M, Perisinakis K, Schandorf C, Fletcher J J and Damilakis J 2016 Pediatric neck multidetector computed tomography: the effect of bismuth shielding on thyroid dose and image quality *Radiat. Prot. Dosim.* **173** 361–73
- [35] Jaya G W and Sutanto H 2018 Fabrication and characterization of bolus material using polydimethyl-siloxane *Mater. Res. Express* **5** 015307
- [36] Mehnati P, Malekzadeh R, Sooteh M Y and Refahi S 2018 Assessment of the efficiency of new bismuth composite shields in radiation dose decline to breast during chest CT *Egypt. J. Radiol. Nucl. Med.* **49** 1187–9
- [37] Spunei M, Malaescu I, Mihai M and Marin C N 2014 Absorbing materials with applications in radiotherapy and radioprotection *Radiat. Prot. Dosim.* **162** 167–70
- [38] Mahmoud M E, El-Khatib A M, Badawi M S, Rashed A R, El-Sharkawy R M and Thabet A A 2017 Fabrication, characterization and gamma rays shielding properties of nano and micro lead oxide dispersed high density polyethylene composites *Radiat. Phys. Chem.* **145** 160–73
- [39] De Jong W H, Van Och F M, Den Hartog Jager C F, Spiekstra S W, Slob W, Vandebriel R J and Van Loveren H 2002 Ranking of allergenic potency of rubber chemicals in a modified local lymph node assay *Toxicol. Sci.* **66** 226–32